Nitrogen-Doped Graphitized Carbon Electrodes for Biorefractory Pollutant Removal

Thi Xuan Huong Le, Roseline Esmilaire, Martin Drobek, Mikhael Bechelany, Cyril Vallicari, Sophie Cerneaux, Anne Julbe, Marc Cretin

Nitrogen-doped Graphitized Carbon Electrodes for Biorefractory Pollutants Removal

Thi Xuan Huong Le[a,b], Roseline Esmilaire[a], Martin Drobek[a], Mikhael Bechelany[a*], Cyril Vallicari[a], Sophie Cerneaux[a], Anne Julbe[a], Marc Cretin[a*]

[a]Institut Européen des membranes, IEM UMR-5635, Université de Montpellier, ENSCM, CNRS, Place Eugène Bataillon, 34095 Montpellier cedex 5, France.

[b]Van Lang University, 45 Nguyen Khac Nhu, District 1, Ho Chi Minh City, Viet Nam.

*   Corresponding   authors: mikhael.bechelany@umontpellier.fr   and Marc.Cretin@umontpellier.fr

ABSTRACT

A novel material was fabricated by deposition of graphitized Nitrogen-doped Porous Carbon layer (NPC) on commercial Carbon Felt (CF). The NPC was obtained via Atomic Layer Deposition of zinc oxide (ZnO) and its subsequent solvothermal conversion to Zeolitic Imidazolate Framework (ZIF-8) followed by its carbonization under controlled atmosphere. Both physical and electrochemical properties have been evaluated by Scanning Electron Microscopy, X-Ray Diffraction, Energy-Dispersive X-ray spectroscopy, X-ray photoelectron spectroscopy, Raman spectroscopy, nitrogen sorption, contact angle and cyclic voltammetry measurements. The parameters affecting the growth of NPC, such as the amount of ZnO/ZIF-8 material before calcination and thermal treatment temperature have been investigated in details. The versatility of the as-prepared NPC/CF material was assessed by studying: *i)* its adsorption ability and/or *ii)* its behavior as cathode in Electro-Fenton process (EF) for the elimination of a model refractory pollutant (acid orange 7 (AO7)). Once used as adsorbent, the NPC/CF proved good adsorption

capacity with 97 % color removal of initial 0.02 mM dye concentration after 30min. Moreover, the application of such novel cathode could also reduce the cost for EF technology by using lower energy consumption at 0.54 $kWh\,g^{-1}$ TOC. The apparent rate constant (k_{app}~0.8 min^{-1}) obtained for NPC/CF was more than 7 times higher compared to pristine CF commercial electrode, thus leading to more than 90% TOC removal in 8 h. In addition, high reaction efficiency and system durability were attributed to continuous regeneration of the NPC/CF sorption capacity upon total mineralization of the pollutants accumulated at the electrode surface. Results confirmed that the new NPC/CF material behaves as a highly active electrode with attractive adsorption efficiency and at the same time it possess an excellent electrochemical activity in Electro-Fenton (EF) oxidation process for the removal of persistent water pollutants.

INTRODUCTION

Among different Electrochemical Advanced Oxidation Processes (EAOP), Electro-Fenton (EF) system is considered as a highly efficient technology in wastewater treatment, namely for the degradation of refractory pollutants. In fact, EF process allows the elimination of Persistent Organic Pollutants (POPs) via the production and reaction of powerful oxidant hydroxyl radicals (•OH) inducing their total mineralization. The •OH radicals are produced in electrochemically assisted Fenton's reaction involving hydrogen peroxide (H_2O_2) and ferrous iron as indicated in Eq. 1 [1].

$$Fe^{2+} + H_2O_2 \rightarrow Fe^{3+} + OH^- + {}^\bullet OH \tag{1}$$

Since this reaction takes place in acidic medium, it can be alternatively expressed as follows (Eq. 2):

$$Fe^{2+} + H^+ + H_2O_2 \rightarrow Fe^{3+} + H_2O + {}^\bullet OH \tag{2}$$

H_2O_2 is formed via two-electrons oxygen reduction reaction (ORR) (Eq. 3) at the cathode and the efficiency of its production is thus a key parameter of EF process.

$$O_2 + 2H^+ + 2e^- \rightarrow H_2O_2 \tag{3}$$

Hence, the improvement of cathode material in ORR, increasing H_2O_2 production, is of high importance for enhancing the EF process efficiency. Carbon-based electrodes are commonly used as cathodes in oxygen-dissolved solutions to produce H_2O_2. In a form of commercial carbon felts (CF), they possess numerous advantages including good conductivity, high chemical and thermal stability, decent mechanical integrity and, last but not least, easy hanging and commercial availability at low cost [2-3]. In addition, the CF enables an efficient regeneration of Fe^{2+} ($Fe^{3+} + e^- \rightarrow Fe^{2+}$), thus making it a very attractive cathode material in EF process [4-6]. In order to upgrade the performance of commercial CF in ORR, various strategies have been proposed including cathode modification by thermal treatment [7] or deposition of carbon-based additives such as graphene [8-9].

Recently, porous carbon (pC) derived from Metal-Organic Frameworks (MOFs) has emerged as an effective material for a variety of applications including capacitive deionization [10], CO_2 adsorption [11], fuel-cells [12], and electrochemical applications [13]. Several pCs have been reported originating from different MOF types, including MOF-5 ($Zn_4O(OOCC_6H_4COO)_3$) [14], zeolitic imidazolate framework (ZIF-8) [10, 13], isoreticular metal-organic framework-3 (IRMOF-3) [15], MOF-199 [16], *etc*. The pC material is typically obtained by thermal treatment under inert atmosphere forming an ordered and calibrated porous structure with high specific surface area and large pore volume. It has been demonstrated that the doping of pC by nitrogen atoms (i.e. pyridinic-N, pyrrolic-N, and quaternary-N) improved significantly the catalytic activity towards ORR [17-19] by decreasing the adsorption energy of oxygen at the electrode surface [20-22] and enhancing the electro-conductivity. Systems with high activity can thus be derived by coupling the N-doping effect with high electroactive surface area [15]. Furthermore, because of their highly porous structure and high specific surface area, carbon materials are also known as adsorbents of high interest for wastewater treatment. For instance, Jiao *et al.* claimed that Co-doped hierarchical porous carbon (Co/HPC) derived from Co/ZIF-8 carbonization is an efficient adsorbent for the extraction of trizine herbicides from wastewater [23]. Nanoporous carbon material obtained by direct carbonization of ZIF-8 was also used as adsorbent for the removal of heavy metal ions from aqueous media [24].

A large number of approaches have been reported in the literature to produce pC materials from MOFs: *i)* thermolysis combined with HF treatment in aqueous solution [24-25]; *ii)* microwave-assisted KOH activation [26]; *iii)* carbonization in presence of alcohols [27]; *iv)* direct carbonization/pyrolysis under inert atmosphere [16, 28-29]. However, most of these studies just focussed on a direct application of the as-formed porous carbon powders, while the deposition/growth of pC on different substrates is scarce. For electrochemical applications, electrodes have been modified in slurries containing C/carbon black and polytetrafluoroethylene (PTFE) [25-26, 28]. The usage of PTFE as a binder may however lead to some disadvantages like

weak adhesion onto the electrode surface, low conductivity of the composite, and limited pC loading [30].

For the sake of overcoming such bottlenecks, in this study, we investigated a novel electrode material fabricated by deposition of graphitized nitrogen-doped porous carbon layer (NPC) on commercial carbon felt (CF). The novelty of the present study bears on the possibility to grow homogeneously the pC precursor on a large variety of substrates with different size, shape, porosity and morphology. The synthesis strategy is based on atomic layer deposition (ALD) of a metal oxide (e.g. ZnO) and its solvothermal conversion to the corresponding MOFs (e.g. ZIF-8), followed by a thermal treatment under inert atmosphere for the formation of pC. It must be noted that the NPC/CF material has a hierarchical structure composed of both macropores providing access of the polluted solution inside the CF structures, and micropores increasing the specific surface area of the electrode. In addition, the N-doping of pC ensures an increase of electro-conductivity. This, coupled with high electroactive surface area should minimize the energy cost of the developed NPC/CF system.

The as-prepared NPC/CF electrode was employed as multifunctional material acting as both adsorbent and active cathode in EF process for the destruction of AO7 as a model refractory water pollutant. It is of particular interest that coupling both adsorption and EF oxidation could maximize the process efficiency as EF helps to continuously regenerate the NPC/CF sorption capacity by total mineralization of the pollutants accumulated on electrode surface. We believe that such a versatile approach, enabling possible synthesis of various pC on numerous electrode substrates and their subsequent applications in electro-Fenton process, is an attractive way for developing a competitive EF process for the destruction of bio-refractory pollutants from waste waters.

EXPERIMENTAL SECTION

1. Materials

Diethyl zinc (DEZ), $Zn(CH_2CH_3)_2$, (95%), AO7 (Orange II sodium salt), sodium sulphate (anhydrous, 99.0 – 100.5%), iron (II) sulphate hepta-hydrate (99%), and methanol (10 wt%) were obtained from Sigma-Aldrich. The carbon felt was provided by Johnson Matthey Co., Germany. 2-methylimidazole (97%), potassium hexacyanoferrate ($\geq$ 99%) and potassium nitrate ($\geq$ 99%) were bought from Fluka. TOC standard of 1000 mg/L (Sigma-Aldrich) and sodium hydrogen carbonate ($\geq$ 99.5%, ACS, Karlsruhe) were used for calibration. Potassium titanium (IV) oxalate (99.99 %, Alfa Aesar), potassium permanganate (> 99 %), sulfuric acid (95 - 97%), and standard hydrogen peroxide solution ($\geq$ 30% w/w, Sigma-Aldrich) were employed to determine the hydrogen peroxide accumulation in time. The aqueous solutions were prepared using 18.2 MΩcm Milli-Q water (Millipore).

2. Modification of carbon felt by graphitized nitrogen-doped porous carbon

The commercial carbon felt (CF) was first cleaned in an ultrasonic bath with acetone for 2h to remove any adsorbed contaminants, then rinsed with deionized water and dried at 60°C for 24h. Such pretreated carbon felt was denoted as "raw CF". The graphitized nitrogen-doped porous carbon (NPC) layers deposited on raw CF have been prepared by a synthesis protocol described in our previous work [31]. It consists of an original strategy coupling *i)* atomic layer deposition (ALD) of a metal oxide (MO) and *ii)* solvothermal conversion of MO into the corresponding metal organic framework (MOF) followed by its carbonization into porous carbon forming NCP/CF electrodes. The ALD step has been performed using a home-made ALD set-up described elsewhere [32]. The CF was sequentially exposed to diethyl zinc (DEZ), $Zn(CH_2CH_3)_2$, and deionized water, separated by a purge step with dry argon (Ar flow rate of 100 sccm) at 100°C, thus forming a ZnO thin layer onto the CF surface. The characteristics of the ZnO deposits (thickness, crystalline phase, grain/crystallite sizes) were found as insensitive to support morphology. ZnO films with different thicknesses (20, 50, 75 and 100 nm) have been deposited in order to optimise the conversion to ZIF-8 and subsequently the electrochemical performance

of the NCP/CF electrodes obtained after the carbonisation step. The growth of ZnO per cycle has been controlled by measuring the thickness of films deposited on Si-wafer companion substrates placed in the ALD reaction chamber. Solvothermal conversion of ZnO into the corresponding MOF (ZIF-8) has been performed at 100°C for 5h in a closed pressured vessel (Teflon–lined stainless-steel autoclave - 45 mL) containing a solution of 2-methylimidazole (2-mim) in methanol (10 wt%). The thermal treatment (carbonization) of ZIF-8 has been conducted at $1000°C$ for 10h under inert N_2 atmosphere, in order to obtain the nitrogen–doped porous carbon (NPC) layer deposited onto the commercial carbon felt (CF), thus forming NPC/CF cathode.

3. Characterization

The surface elemental composition of the as-prepared electrodes was determined by X-ray Photoelectron Spectroscopy (XPS) on an ESCALAB 250 (Thermo Electron) with Al Kα (1486.6 eV) source. Analyzed surface was 400 µm in diameter and the background signal was removed using the Shirley method [33]. The surface atomic concentrations were determined from photoelectron peaks areas using the atomic sensitivity factors reported by Scofield [34]. Binding energies (BE) of all core levels were referred to C=C of C1s carbon at 284.4 eV. The N_2 adsorption-desorption isotherms were measured using Micromeritics ASAP2010 equipment (out gassing conditions: 200°C-12h in vacuum). Further morphological, chemical and structural characterizations have been performed by scanning electron microscopy (SEM, Hitachi S-4800), a homemade contact angle meter, X-ray diffraction (XRD) (PANAlytical Xpert-PRO diffractometer equipped with a X'celerator detector using Ni-filtered Cu-radiation) and EDX analysis (Silicon Drift Detector (SDD), X-MaxN, Oxford Instrument) coupled to a Zeiss EVO HD15 SEM analyzer. Electrochemical measurements were carried out in a three-electrode cell using a µ3AUT70466 Autolab system (Eco Chemie BV, Netherlands) at room temperature. Cyclic voltammetry (CV) was conducted in a 10 mM $K_3[Fe(CN)_6]$ and 1.0 M KNO_3 solution

with a working electrode (carbon cathode), a counter electrode (Pt foil), and a reference electrode (Saturated Calomel Electrode, SCE).

4. Removal of AO7 by adsorption

Adsorption experiments were performed in a batch experimental set-up containing AO7 solutions with concentrations in the range of 0.02 mM − 0.5 mM. The pH of the solutions was adjusted to ~ 6.8 under magnetic stirring (500 rpm) at room temperature. The decolorization of AO7 pollutant was monitored by measuring the dye absorbance at the selected single wavelength of 485 nm specific to the azo bonds [35] using Spectrophotometer Jenway 6300 (Barioworld Scientific Ltd, Dunmow UK). All experiments were repeated three times, and average values were used for further calculations.

The NPC/CF surface charge was determined with the help of Na_2SO_4 (50 mM) solution (pH = 3.0 to 12.5) adjusted by addition of either sulphuric acid (H_2SO_4) or sodium hydroxide (NaOH) solutions. The NPC/CF was immersed in a stirred solution continuously bubbled with N_2 during experiments in order to avoid any effect of atmospheric CO_2 on the pH of the solutions. At the end of each experiment, the pH was measured in order to monitor the difference between the initial and final pH values.

5. Mineralization of AO7 by electro-Fenton oxidation

The EF experiments were carried out after the adsorption step (equilibrium reached after 2h). Na_2SO_4 (50 mM) as supporting electrolyte and $FeSO_4.7H_2O$ (0.2 mM) as catalyst were added to AO7 solution whose pH was adjusted at ~3 with H_2SO_4 solution (1 M) [4]. At selected time intervals, aliquots of 1 mL were withdrawn and filtered (at 0.2 µm) before measuring the TOC removal with the help of a TOC-L CSH/CSN Shimadzu (Japan). Calibration curves for total carbon (TC) and inorganic carbon (IC) analyses were obtained by automatic dilution of standards solutions of TOC (potassium hydrogenophtalate) and IC (sodium hydrogen carbonate).

The specific energy consumption per unit TOC mass (EC$_{TOC}$) was calculated according to Eq. (4) [36]:

$$EC_{TOC} \text{ (kWh g}^{-1}\text{ TOC)} = \frac{VIt}{\Delta(TOC)_{exp}V_s} \quad (4)$$

where V is the average cell voltage (V), V$_s$ the solution volume (L), $\Delta(TOC)_{exp}$ is the experimental TOC decay (mg L^{-1}), I the applied current (A) and t the electrolysis time (h).

RESULTS AND DISCUSSION

1. Synthesis and characterization of NPC/CF

As specified in the experimental part, the graphitized nitrogen-doped porous carbon material deposited on commercial carbon felts (NPC/CF) was fabricated by combining *i)* Atomic Layer Deposition (ALD) of metal oxide (ZnO) and *ii)* solvothermal conversion of ZnO to ZIF-8, followed by its subsequent carbonisation under controlled atmosphere. The number of ALD cycles has been adjusted in order to control the ZnO layer thickness as reported elsewhere [37]. After the solvothermal conversion of ALD modified carbon felts, a ZIF-8-based composite material has been obtained on the CF surface (Figure 1a). The SEM images of the CF@ZIF-8/ZnO composites are shown in Figures 1b and 1c, revealing homogeneous coverage of the carbon fibers with ZIF-8 crystals having typical rhombic dodecahedron shape [13, 38]. When carbonized in controlled atmosphere, this composite material transforms into nitrogen-doped porous carbon (NPC) thin layer on the CF surface (Figures 1d and 1e). In a good agreement with the literature [17], the NPC preserved the original polyhedral shape of ZIF-8 (Figure 1f). The EDX mapping (Figures 1g to 1j) clearly evidenced the presence of C, N and O atoms *(C 88.9 at%, N 7.3 at%, O 3.6 at%)*, proving the formation of nitrogen-doped carbon.
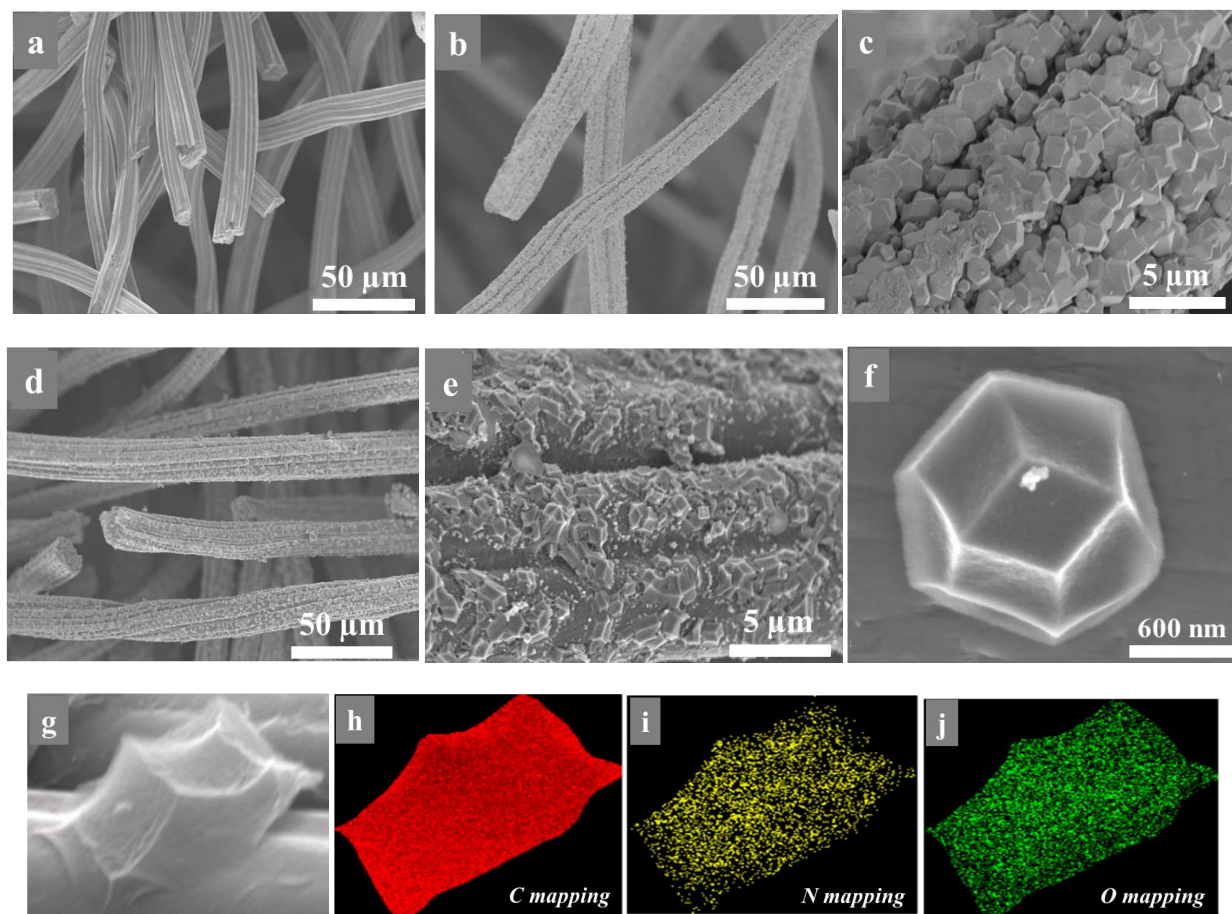
Figure 1. SEM images of (a) raw CF; (b, c) CF@ZIF-8/ZnO composite; (d, e) NPC/CF; (f, g) single porous nitrogen-doped carbon particle; and (h, i, j) EDX mapping of NPC/CF.

Nitrogen-doping of the porous carbon thin layer deposited on CF was proven by the deconvolution of high-resolution XPS spectrum in N1s region (Figure 2). The appearance of nitrogen in NPC/CF could be attributed to N-containing functional groups such as pyridinic-N (398.2 eV), pyrrolic-N (399.8 eV), quaternary-N (400.8 eV) and N-oxide (403 eV) [11, 13]. These nitrogen-containing groups are expected to enhance surface hydrophilicity and thus to promote mass transfer between the NPC/CF and the electrolyte. Such characteristic, coupled to the enhanced electron transport and high surface area, should improve the electrochemical performance of the system in ORR during EF process [17, 39].
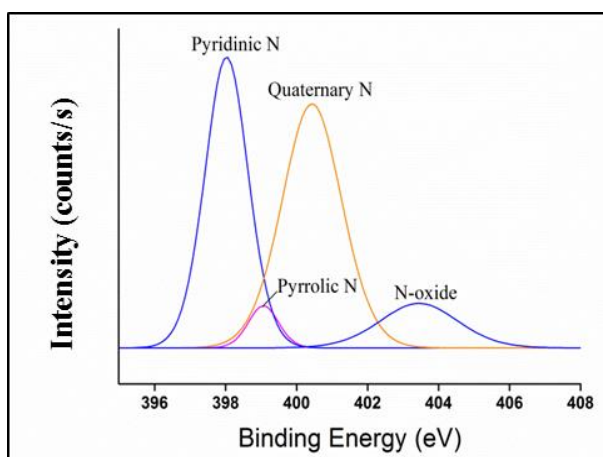
Figure 2. N1s spectrum of NPC/CF (from XPS analysis).

2. Influence of the synthesis parameters on NPC/CF characteristics

2.1. Thickness of ZnO layer

The initial thickness of ZnO layers has been modulated in the range 20-100 nm by controlling the number of ALD cycles, while other reaction parameters including solvothermal conversion and carbonization steps were kept constant. The electrochemical performance of the NPC/CF as a function of initial ZnO thickness has been evaluated by running cyclic voltammetry (CV) measurements in a 10 mM $K_3[Fe(CN)_6]$ and a 1.0 M KNO_3 solution. The current response of the modified electrode towards $[Fe(CN)_6]^{3-/4-}$ increased with increasing ZnO thickness (Figure 3d). This phenomenon was attributed to the higher quantity of ZIF-8 obtained by solvothermal conversion of ZnO-richer samples, leading to crystal oriented growth and non-compact stacking [38], thus yielding higher quantity of NPC after carbonisation. According to N_2 physisorption measurements, the specific surface area increased by more than 64 times for NPC/CF sample with ZnO thickness at 100 nm in comparison with raw CF carbon felts (0.09 m²g⁻¹). The increase of ZnO thickness induces the increase of the specific surface area (S_{BET}) (Table S1) of the final NPC/CF electrode resulting from a higher amount of ZIF-8 formed after the solvothermal conversion step. In fact, the amount of NPC and thus the active surface is raised gradually as a function of the initial ZnO thickness. The NCP-covered carbon felts obtained after the conversion and carbonisation of samples with different initial amounts of ZnO are shown in

Figures 3a, b and c. Comparing the activity of pristine and NPC/CF electrodes in CV measurements evidenced a significant increase of the current density in the case of NCP-modified electrodes, thus proving their promising potential for electrochemical applications.
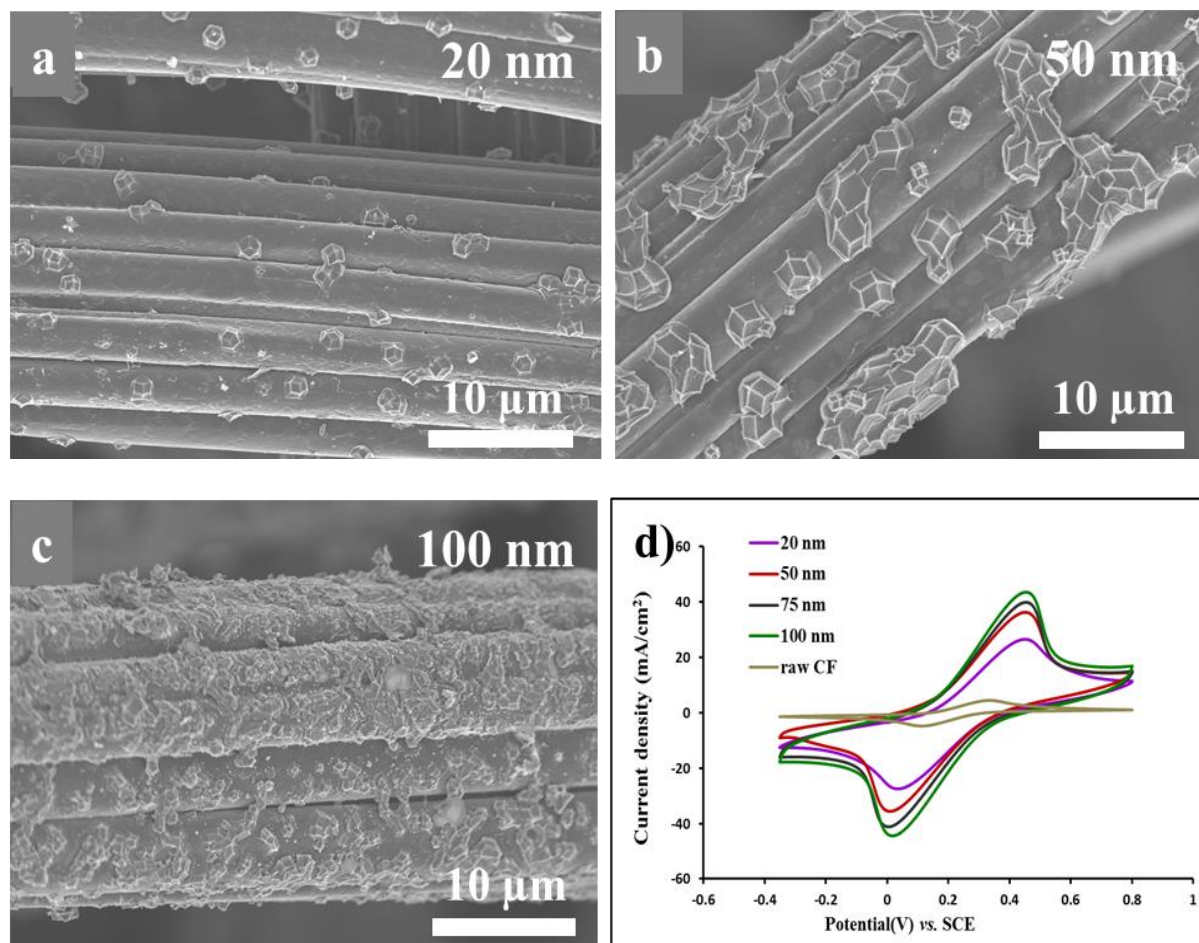

Figure 3. SEM images of NPC/CFs obtained from samples with different initial ZnO thicknesses: (a) 20 nm, (b) 50 nm, (c) 100 nm; (d) CV curve of raw CF and NPC/CF materials obtained from samples with 20, 50, 75, 100 nm initial ZnO thickness. CV conditions: potassium hexacyanoferrate solution (10 mM) in 1 M KNO_3. Scan rate of 7 $mV.s^{-1}$.

2.2. Carbonisation treatment

In order to investigate the effect of carbonisation treatment conditions, series of NPC/CF samples with 100 nm initial ZnO thickness (i.e. exhibiting the highest current density in CV measurements) were prepared by pyrolysing the ZIF-8 at different temperatures and times. Thermogravimetric analysis of the CF@ZIF-8/ZnO composites (Figure 4b) revealed that

carbonization starts at 600 °C. Sample series were thus prepared by applying 10 h pyrolysis treatment in the temperature range 600-1200°C. The CV curves (Figure 4a) reveal that the current density increases with the pyrolysis temperature up to 1000°C. Above this temperature, virtually-zero improvement of electrochemical performance was detected. This phenomenon could be attributed to the progressive extraction of metallic Zn from the ZIF-8 structure during the carbonization process and its subsequent complete vaporization at ~ 1000°C (the boiling point of Zn being ~ 908 °C) [17].

The effect of the calcination time at 1000°C has been evaluated in the range from 30 min up to 24h. The CV curves (Figure 4d) shows that the current densities raised gradually and the anodic and cathodic peaks separation was smaller when the pyrolysis time at 1000°C increased from 30 minutes to 10h. In fact, sufficiently long carbonization time is required at 1000°C in order to achieve full conversion of ZIF-8 to porous carbon, with complete Zn removal and NPC crystallization [40-41]. On the other hand, further prolongation of the thermal treatment tend to decline the NPC/CF performance (Figure 4d) by decreasing the current density on the redox probe $[Fe(CN)_6]^{3-}/[Fe(CN)_6]^{4-}$ nearly twice for the 24 h pyrolysed sample. This could be explained by a possible collapse of the NPC porous structure. Indeed a large extent of collapse of the carbon skeleton has been reported in the literature when the temperature is increased above 900°C [42]. In addition, long-term thermal treatment at 1000°C could also accelerate the decomposition of the N-containing carbon framework, resulting in a lower N content and/or collapsed porous structure. As shown in Figure 4c, the polyhedral NPC particles are no more observed, although a granular carbon layer uniformly covers the CF surface (Figure 4c).
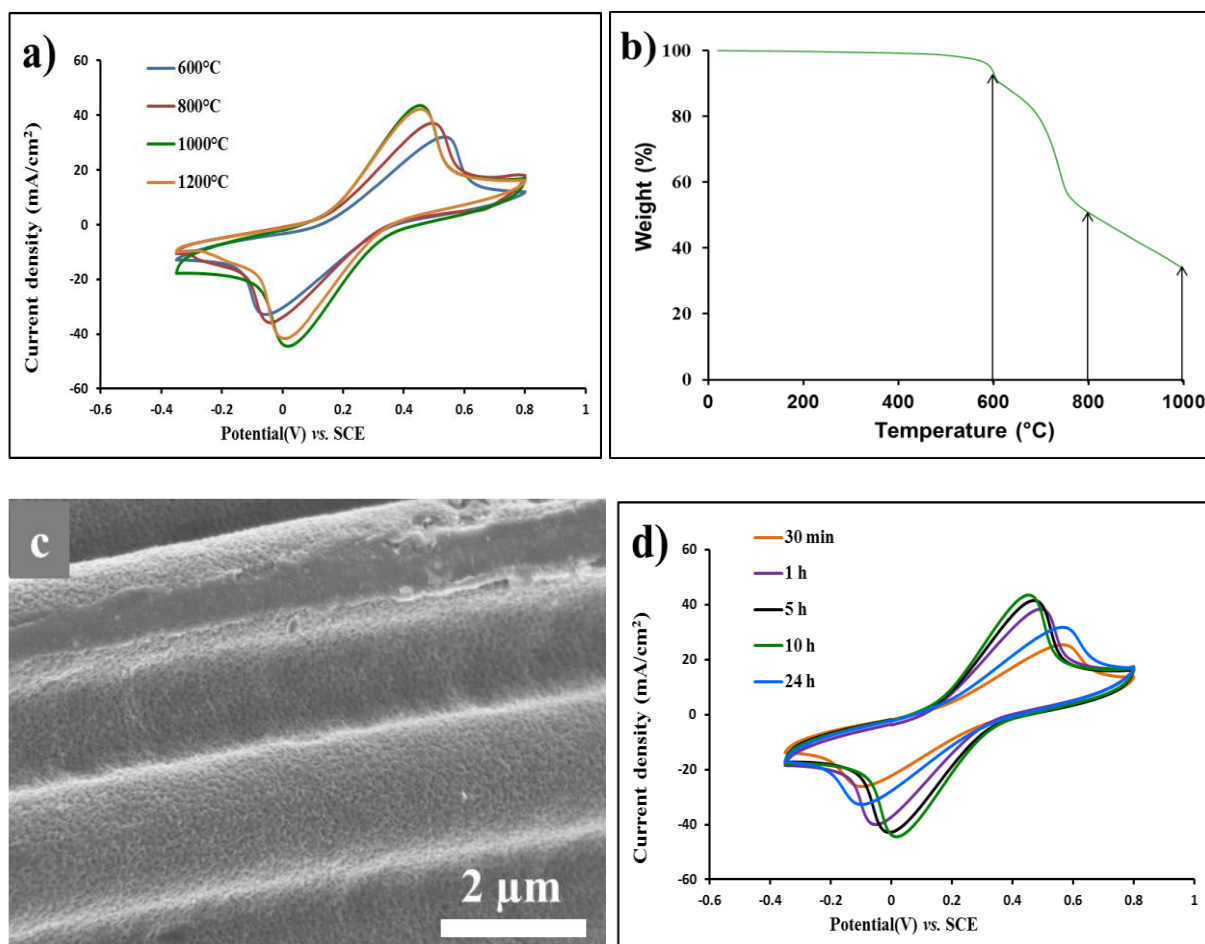
Figure 4. (a) CV curves of NPC/CFs prepared at various temperatures, (b) TGA of CF@ZIF-8/ZnO composite material under N_2, 5°C/min, (c) SEM image of NPC/CF after 24 h thermal treatment, and (d) CV curves of NPC/CFs calcined at 1000°C and different heating times. CV conditions: potassium hexacyanoferrate solution (10 mM) in 1 M KNO_3. Scan rate 7 mV s^{-1}.

3. Adsorption capacity of NPC/CF

Owing to its hierarchical porous structure, with both high surface area and open porosity, the NPC/CF material is potentially a relevant adsorbent for the elimination of water pollutants. The efficiency of NPC/CF for removing dye pollutants such as AO7 is demonstrated in Figure 5a for dye concentrations in the range 0.02 mM - 0.5 mM. As expected, the adsorbent efficiency declined with increasing dye concentration due to saturation of adsorption sites on the NPC/CF surface [43-44]. At low concentration (0.02 mM), over 97% of AO7 was removed after 30 min while only 8% abatement was achieved for the most concentrated solution (0.5 mM). This

observation is in line with the results published by Lim *et al.* for zeolite-activated carbon macrocomposites and showing a 6-folds adsorption decrease when the initial AO7 dye concentration increased from 100 to 400 mg/L [45]. As shown in Figure 5a, dye adsorption is very fast at the beginning of the process, and reached equilibrium after 60 min for all concentrations.

To shed further light on the dye adsorption mechanism, experimental data were analyzed with the help of well-known Langmuir and Freundlich models. The Langmuir adsorption isotherm predicts a monolayer adsorption on specific sites. The Langmuir equation is expressed as follows (Eq. 5)

$$\frac{C_e}{Q_e} = \frac{1}{Q_m K} + \frac{C_e}{Q_m} \tag{5}$$

where Q_e is the amount adsorbed ($\mu g.cm^{-2}$); C_e is the equilibrium dye concentration ($\mu g.L^{-1}$); Q_m and K are Langmuir constants related to the maximum adsorption capacity and the free energy of adsorption, respectively.

The Freundlich isotherm is an empirical equation employed to describe heterogeneous systems. The logarithmic form of Freundlich model is given by Equation 6:

$$log Q_e = log K_f + (1/n) log C_e \tag{6}$$

where K_f and n are Freundlich adsorption isotherm constants, being indicative of the adsorption extent and the degree of non-linearity between solution concentration and adsorption, respectively.

Figures 5c and 5d reveal that the AO7 adsorption on NPC/CF material fits Langmuir isotherm with higher correlation coefficient ($R^2=0.9998$) in comparison to Freundlich isotherm ($R^2=0.7941$). Such results correspond well to those published elsewhere on other adsorbing materials [46-48] and confirm that the adsorption process fits the monolayer adsorption model.

Another important parameter influencing adsorption efficiency is the solution pH. The results plotted in Figure 5b reveals that the pH of a 50 mM Na_2SO_4 solution remains unchanged after 2h immersion of the NPC/CF in a solution at pH $\leq$ 7. Over this value, the pH tends to decrease. Such results confirm that the surface of NPC/CF material is positively charged, and is thus able to attract negative molecules like AO7 dye in aqueous medium. The positive charge of

NPC/CF surface could be linked to the presence of nitrogen species. These charge effects also contribute to fasten initial adsorption kinetics observed in Figure 5a: at high initial AO7 concentration, the material active sites quickly saturate and the dye removal efficiency decreases remarkably. The NPC/CF material proved high adsorption capacity as its performance (calculated from Langmuir isotherm) is over 18 times higher than the value reported for zeolite-activated carbon macrocomposites [45].
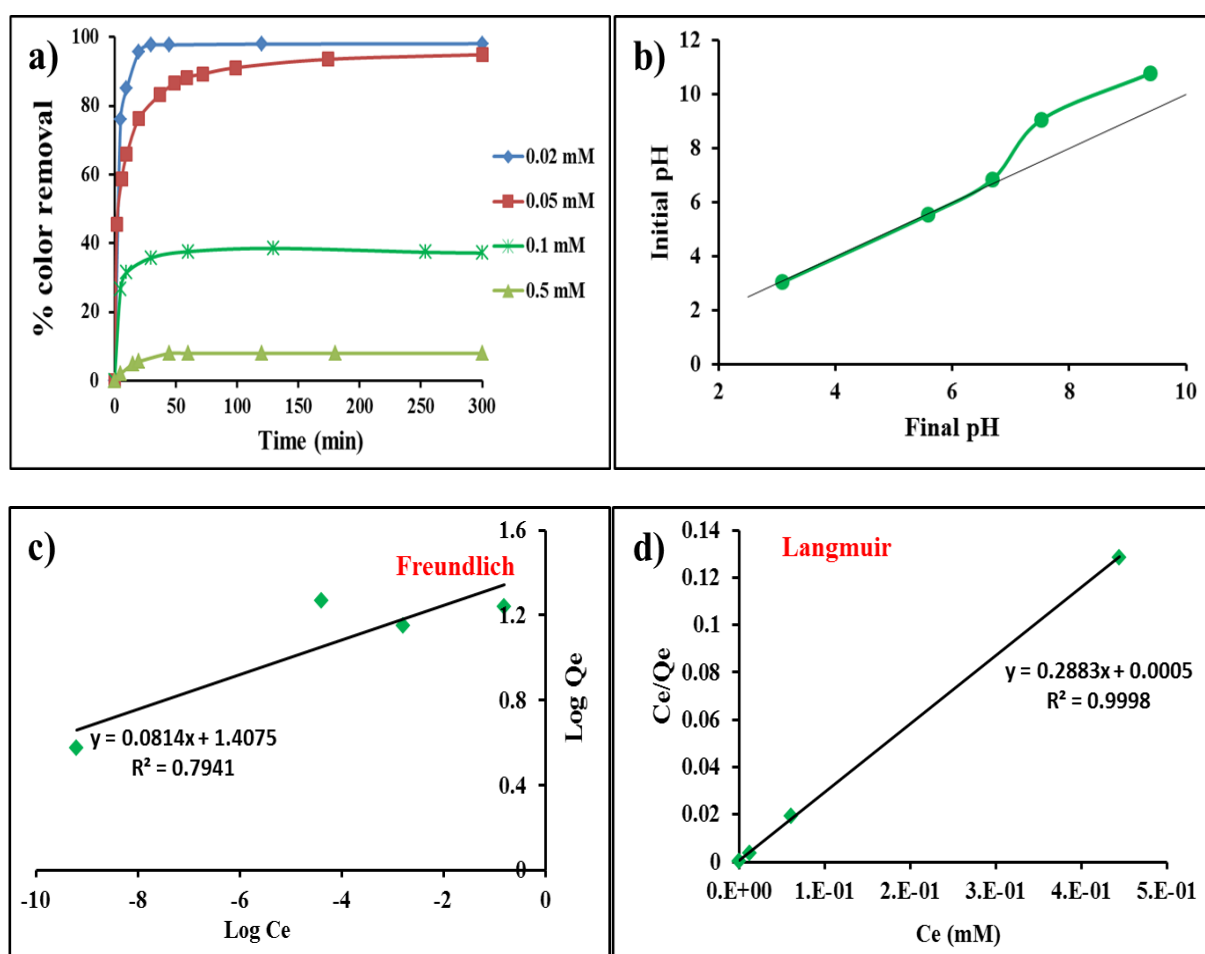

Figure 5. (a) Evolution of the % color removal at various AO7 dye concentrations, (b) pH variation in Na_2SO_4 solution after immersing NPC/CF material for 2h, (c) Freundlich adsorption isotherm, and (d) Langmuir adsorption isotherm.

On the other hand, the AO7 dye adsorption virtually did not occur on raw commercial CF. This phenomenon could be attributed to both the hydrophobic property of raw CF (water

contact angle ~89.9°) and to its low specific surface area (0.09 m^2g^{-1}). Contrarily, the NPC/CF containing N-based groups is covered with hydrophilic spots that help to drag AO7 molecules into the macroporous network of the carbon felt. At the same time, its high specific surface area ensures an effective adsorption of dye molecules. The full saturation is reached once all active sites in NPC/CF are filled with dye molecules. It can be concluded that due to its high surface area, high accessible porosity, and positively charged surface nitrogen groups, the NPC/CF material has a high adsorption capacity for the abatement of negatively-charged water pollutants. In general, the main bottleneck limiting long-term application of adsorption-based processes bears on problematic sorbent regeneration for avoiding full saturation. In order to address this issue, a coupling of adsorption with electro-Fenton process technology has been considered in the next section.

4. System coupling electron-Fenton and adsorption processes

As described in the experiment part, the EF experiments were carried out after immerging the NPC/CF cathode in a 0.1 mM AO7 solution. As evidenced in Figure 6a, the removal of AO7 by the effect of adsorption reached more than 35% within 30 min. When the adsorption equilibrium was attained (after 2 hours), iron catalyst was added to the system in order to run the EF process. As shown in Figure 6, the AO7 dye has been eliminated within 7 and 60 minutes when using either NPC/CF or raw CF, respectively. The apparent rate constant (k_{app}) [4, 6, 49], reaching values ~0.8 min^{-1} for NPC/CF, was more than 7 times higher in comparison with the value for raw CF. In addition, from Figure 6b it is clear, that TOC removal was ~90% after 8h with NPC/CF, while it did not overpass 60% for raw CF. Such outstanding performance could be ascribed to both high electroactive surface area and enhanced conductivity of NPC/CF material. Indeed, the higher conductivity of NPC/CF (Figure S1) promotes faster electron transport, leading to the production of higher amount of H_2O_2 by oxygen reduction reaction (ORR) [50], and thus higher amounts of hydroxyl radicals ($^{\bullet}OH$) as highly oxidizing agent. In contrast, in the case

of raw CF, the EF reaction is less pronounced because of both lower conductivity and poor hydrophilicity of the electrode. The raw CF exhibits poor electrochemical properties because of higher interfacial charge-transfer resistance (R_{ct}) which was evidenced by the measurements of electrochemical impedance spectroscopy (Figure S1). R_{ct} (inversely proportional to the exchange current density, j_0) is related to the number of electrons that are transferred from the catalytic surface to the reactant(s). The bigger is R_{ct}, the lower is the kinetic rate. Thus, R_{ct} should be as small as possible to enable a fast electrochemical kinetics. The decrease of R_{ct} from 2.4 Ω to 0.7 Ω for raw CF and NPC/CF respectively can then be explained by an increase of the active sites density caused by enhanced real electroactive surface area induced by the presence of the microporous carbon layer on the surface of CF. The excellent properties of NPC/CF for H_2O_2 production could be also explained by delocalized conjugated system with the sp^2-hybridized nitrogen-doped carbon framework with lone electron pairs resulting in improved ORR performance [17, 39, 51]. This finding, revealing improved EF process efficiency in terms of lower energy consumption (E_c), has also strong impact on the cost of EF treatment. The E_c value for NPC/CF was around 0.54 kWh g^{-1} TOC instead of 1.08 kWh g^{-1} TOC for raw CF, leading thus to 50% reduction of the total energy consumption. As summarized on Table 1, the reduction of E_c value was also 1.7 times and 1.4 times higher for NPC/CF in comparison with electrodes based on graphene/carbon felt and graphene/carbon cloth, respectively. Concerning the synthesizing method, the fabrication process is simple including two uncomplicated steps: (1) Atomic Layer Deposition of zinc oxide (ZnO) followed by its subsequent solvothermal conversion to Zeolitic Imidazolate Framework (ZIF-8) and (2) the carbonization of the as-prepared material. Such synthesis protocol is very robust and does not require any strict synthesis conditions or a high quantity of expensive chemicals. The proposed method enables designing of a new material (electrode) with an outstanding electrochemical performance and long-term stability. It is applicable for biorefractory pollutants removal featuring both adsorption and electrochemical activity in electro-Fenton process. In comparison with conventional porous

carbon (PC) of graphene layer deposited onto the commercial carbon felt (CF), the synthesis/application of the novel NPC/CF electrode proposed in this work presents several advantages: (i) The synthesis method of NPC/CF electrode does require any strict control of gas flow during thermal treatment. In contrast, to form the conventional porous carbon (PC), it is necessary to apply a mixture of N_2/O_2 with well-defined composition. If the oxygen ratio exceeds an optimal value, carbon felt (CF) would be damaged (destroyed). Moreover, the method applied for the formation of conventional porous carbon (PC), does not allow an insertion of functional nitrogen groups which are important catalytic sites for oxygen reduction reaction (ORR) during electro-Fenton process. (ii) Better stability of NPC/CF electrode in comparison with graphene-modified CFs which sufferer from leaching of graphene into the solution during electrochemical process. It has been evidenced in previous studies that the TOC removal after 5 EF cycles decreased by 5.4% for graphene-CF [9], and 21 % for Graphene/Carbon cloth[52].

Last but not least, the NPC/CF cathode proved significant stability after multiple reaction cycles. The TOC removal decreased by 5.4% only after 10 subsequent reaction cycles (Figure 6b). A slight decline of electrochemical performance was also observed when running the CV measurements in potassium hexacyanoferrate (Figure S2). This phenomenon was probably caused by a partial detachment of the NPC layer during the washing process conducted with deionized water. However, such decline of the TOC removal after long term operation and multiple cycling tests can be considered as negligible, in comparison with the high efficiency of the EF oxidation process.

Table 1. Mineralization efficiency of EF process applying diverse cathode materials.

Cathode material	Pollutant	% TOC removal increase*	% TOC removal decrease†	%E_c decrease‡	Ref
Graphene/Carbon felt	AO7	33	6	29	9
Chemically	p-nitrophenol	29	5	n/a	17

modified graphite felt					
Graphene/Carbon cloth	Phenol	51	21	36	52
Thermally treated carbon felt	Paracetamol	31	1	-	7
NPC/CF	AO7	42	3	50	**This work**

*compared to raw cathode after 2 h treatment
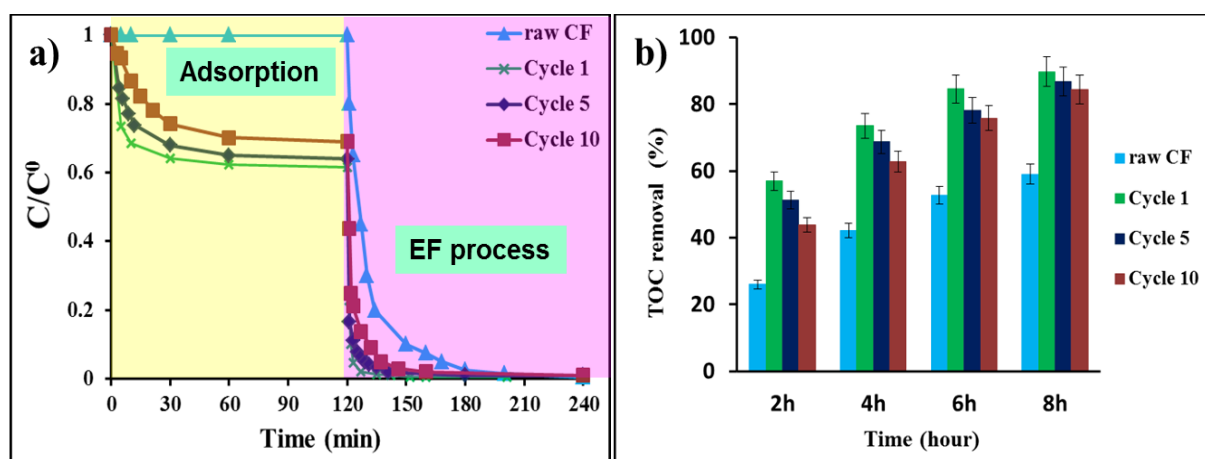†after 5 cycles
‡compared to bare CF cathode

Figure 6. (a) Kinetics of AO7 removal by both adsorption and electro-Fenton processes.

(b) TOC removal after 8h; Conditions: V=50 mL, [AO7]=0.1 mM; $[Fe^{2+}]$=0.2 mM; pH=3;

$[Na_2SO_4]$=50 mM, I = 25 mA; anode: Pt, cathode: raw CF and NPC/CF.

CONCLUSION

In this study, commercial carbon felts were modified by nitrogen-doped porous carbon, aiming to develop versatile carbon-based electrodes for efficient abatement of water pollutants by coupling adsorption and electron-Fenton processes. The modification has been realized by applying a synthesis strategy based on *i)* atomic layer deposition (ALD) of ZnO and *ii)* solvothermal conversion of ZnO into corresponding ZIF-8 followed by its carbonisation treatment forming the NCP/CF electrode. Key parameters influencing the growth of nitrogen-doped porous carbon layers were investigated, including ZnO thickness, temperature and duration of thermal treatment (carbonisation step). It has been demonstrated that the proposed

surface modification increases hydrophilicity, conductivity and electrocatalytic activity of commercial carbon felts. The derived NPC/CF electrode was used for coupling adsorption and electro-Fenton processes in order to eliminate a model pollutant (AO7) from aqueous medium. The percentage of adsorption reached over 97 % of initial 0.02 mM dye concentration after 30 min. During the EF process, 90% TOC removal has been achieved within 8 h and the apparent rate constant (k_{app}~0.8 min^{-1}) was more than 7 times higher compared to pristine CF commercial electrode. Moreover, the NPC/CF cathode proved lower energy consumption (0.54 kWh g^{-1} TOC) compared to raw CF. At the same time, the NPC/CF electrode exhibited high reaction efficiency and system durability due to continuous regeneration of the NPC/CF sorption capacity by total mineralization of pollutants accumulated on its surface. Thanks to the versatility of the proposed protocol, enabling the synthesis of various MOFs and their subsequent carbonisation into specific porous carbons, many different electrode architectures can be possibly designed for applications in both environmental and energy-related areas. Different studies are currently under progress in these areas and will be reported in next communications.

SUPPORTING INFORMATION

Figure S1. Electrochemical impedance spectroscopy (EIS) of raw CF and NPC/CF electrodes. Figure S2. CVs of NPC/CF after 5 and 10 running cycles. Table S1. Surface area of raw CF and NPC/CF materials obtained from samples with different initial ZnO thickness.

ACKNOWLEDGMENTS

REFERENCES

1. Rodrigo, M. A.; Oturan, N.; Oturan, M. A. Electrochemically Assisted Remediation of Pesticides in Soils and Water: A Review. *Chem Rev* **2014,** *114*, 8720-45.
2. J. González-García; P. Bonete; E. Expósito; V. Montiel; A. Aldaz; Torregrosa-Maciá, R. Characterization of a Carbon Felt Electrode: Structural and Physical Properties. *Journal of Materials Chemistry* **1999,** *9*, 419-426.
3. E. Brillas; I. Sirés; Oturan, M. A. Electro-Fenton Process and Related Electrochemical Technologies Based on Fenton's Reaction Chemistry. *Chem Rev* **2009,** *109* 6570–6631.
4. Ozcan, A.; Oturan, M. A.; Oturan, N.; Sahin, Y. Removal of Acid Orange 7 from Water by Electrochemically Generated Fenton's Reagent. *J Hazard Mater* **2009,** *163*, 1213-20.
5. Panizza, M.; Oturan, M. A. Degradation of Alizarin Red by Electro-Fenton Process Using a Graphite-Felt Cathode. *Electrochimica Acta* **2011,** *56*, 7084-7087.
6. Diagne, M.; Oturan, N.; Oturan, M. A. Removal of Methyl Parathion from Water by Electrochemically Generated Fenton's Reagent. *Chemosphere* **2007,** *66*, 841-8.
7. Le, T. X. H.; Charmette, C.; Bechelany, M.; Cretin, M. Facile Preparation of Porous Carbon Cathode to Eliminate Paracetamol in Aqueous Medium Using Electro-Fenton System. *Electrochimica Acta* **2016,** *188*, 378-384.
8. Thi Xuan Huong Le; Mikhael Bechelany; Joffrey Champavert; Cretin, M. A Highly Active Based Graphene Cathode for the Electro-Fenton Reaction. *RSC Adv.* **2015,** *5*, 42536.
9. Le, T. X. H.; Bechelany, M.; Lacour, S.; Oturan, N.; Oturan, M. A.; Cretin, M. High Removal Efficiency of Dye Pollutants by Electron-Fenton Process Using a Graphene Based Cathode. *Carbon* **2015,** *94*, 1003-1011.
10. Duan, X.; Liu, W.; Chang, L. Porous Carbon Prepared by Using Zif-8 as Precursor for Capacitive Deionization. *Journal of the Taiwan Institute of Chemical Engineers* **2016,** *62*, 132-139.
11. Ma, X.; Li, L.; Wang, S.; Lu, M.; Li, H.; Ma, W.; Keener, T. C. Ammonia-Treated Porous Carbon Derived from Zif-8 for Enhanced Co2 Adsorption. *Applied Surface Science* **2016,** *369*, 390-397.
12. I.A. Khan; A. Badshah; N. Haider; S. Ullah; D.H. Anjum; Nadeem, M. A. Porous Carbon as Electrode Material in Direct Ethanol Fuel Cells (Defcs) Synthesized by the Direct Carbonization of Mof-5. *Journal of Solid State Electrochemistry* **2014,** *18*, 1545–55.
13. Jiang, M.; Cao, X.; Zhu, D.; Duan, Y.; Zhang, J. Hierarchically Porous N-Doped Carbon Derived from Zif-8 Nanocomposites for Electrochemical Applications. *Electrochimica Acta* **2016,** *196*, 699-707.
14. Hu, J.; Wang, H.; Gao, Q.; Guo, H. Porous Carbons Prepared by Using Metal–Organic Framework as the Precursor for Supercapacitors. *Carbon* **2010,** *48*, 3599-3606.
15. Fu, S.; Zhu, C.; Zhou, Y.; Yang, G.; Jeon, J.-W.; Lemmon, J.; Du, D.; Nune, S. K.; Lin, Y. Metal-Organic Framework Derived Hierarchically Porous Nitrogen-Doped Carbon Nanostructures as Novel Electrocatalyst for Oxygen Reduction Reaction. *Electrochimica Acta* **2015,** *178*, 287-293.
16. Raoof, J.-B.; Hosseini, S. R.; Ojani, R.; Mandegarzad, S. Mof-Derived Cu/Nanoporous Carbon Composite and Its Application for Electro-Catalysis of Hydrogen Evolution Reaction. *Energy* **2015,** *90*, 1075-1081.
17. Zhang, L.; Su, Z.; Jiang, F.; Yang, L.; Qian, J.; Zhou, Y.; Li, W.; Hong, M. Highly Graphitized Nitrogen-Doped Porous Carbon Nanopolyhedra Derived from Zif-8 Nanocrystals as Efficient Electrocatalysts for Oxygen Reduction Reactions. *Nanoscale* **2014,** *6*, 6590-602.
18. Yuan, W.; Li, J.; Xie, A.; Chen, P.; Li, S.; Shen, Y. Practical, Cost-Effective and Large-Scale Production of Nitrogen-Doped Porous Carbon Particles and Their Use as Metal-Free Electrocatalysts for Oxygen Reduction. *Electrochimica Acta* **2015,** *165*, 29-35.
19. Yuanfu Deng; Ye Xie; Kaixiang Zou; Ji, X. Review on Recent Advances in Nitrogen-Doped Carbons: Preparations and Applications in

Supercapacitors. *J. Mater. Chem. A* **2016,** *4*, 1144.

20. H. Zhong; C. Deng; Y. Qiu; L. Yao; Zhang, H. Nitrogen-Doped Hierarchically Porous Carbon as Efficient Oxygen Reduction Electrocatalysts in Acid Electrolyte. *J. Mater. Chem. A* **2014,** *2*, 17047–17057.

21. Luo, Z.; Lim, S.; Tian, Z.; Shang, J.; Lai, L.; MacDonald, B.; Fu, C.; Shen, Z.; Yu, T.; Lin, J. Pyridinic N Doped Graphene: Synthesis, Electronic Structure, and Electrocatalytic Property. *Journal of Materials Chemistry* **2011,** *21*, 8038.

22. Takashi Ikeda; Mauro Boero; Sheng-Feng Huang; Kiyoyuki Terakura; Masaharu Oshima; Ozaki, J. Carbon Alloy Catalysts: Active Sites for Oxygen Reduction Reaction. *J. Phys. Chem. C* **2008,** *112*, 14706-14709.

23. Jiao, C.; Li, M.; Ma, R.; Wang, C.; Wu, Q.; Wang, Z. Preparation of a Co-Doped Hierarchically Porous Carbon from Co/Zn-Zif: An Efficient Adsorbent for the Extraction of Trizine Herbicides from Environment Water and White Gourd Samples. *Talanta* **2016,** *152*, 321-8.

24. Bakhtiari, N.; Azizian, S.; Alshehri, S. M.; Torad, N. L.; Malgras, V.; Yamauchi, Y. Study on Adsorption of Copper Ion from Aqueous Solution by Mof-Derived Nanoporous Carbon. *Microporous and Mesoporous Materials* **2015,** *217*, 173-177.

25. Yan, X.; Li, X.; Yan, Z.; Komarneni, S. Porous Carbons Prepared by Direct Carbonization of Mofs for Supercapacitors. *Applied Surface Science* **2014,** *308*, 306-310.

26. Yu, M.; Zhang, L.; He, X.; Yu, H.; Han, J.; Wu, M. 3d Interconnected Porous Carbons from Mof-5 for Supercapacitors. *Materials Letters* **2016,** *172*, 81-84.

27. Liu, B.; Shioyama, H.; Jiang, H.; Zhang, X.; Xu, Q. Metal–Organic Framework (Mof) as a Template for Syntheses of Nanoporous Carbons as Electrode Materials for Supercapacitor. *Carbon* **2010,** *48*, 456-463.

28. Yi, H.; Wang, H.; Jing, Y.; Peng, T.; Wang, X. Asymmetric Supercapacitors Based on Carbon Nanotubes@Nio Ultrathin Nanosheets Core-Shell Composites and Mof-Derived Porous Carbon Polyhedrons with Super-Long Cycle Life. *Journal of Power Sources* **2015,** *285*, 281-290.

29. Zou, G.; Jia, X.; Huang, Z.; Li, S.; Liao, H.; Hou, H.; Huang, L.; Ji, X. Cube-Shaped Porous Carbon Derived from Mof-5 as Advanced Material for Sodium-Ion Batteries. *Electrochimica Acta* **2016,** *196*, 413-421.

30. Lv, Z.; Chen, Y.; Wei, H.; Li, F.; Hu, Y.; Wei, C.; Feng, C. One-Step Electrosynthesis of Polypyrrole/Graphene Oxide Composites for Microbial Fuel Cell Application. *Electrochimica Acta* **2013,** *111*, 366-373.

31. Thi Xuan Huong Le; Roseline Esmilaire; Martin Drobek; Mikhael Bechelany; Cyril Vallicari; Duy Linh Nguyen; Anne Julbe; Sophie Tingry; Cretin, M. Design of a Novel Fuel Cell-Fenton System: A Smart Approach to Zero Energy Depollution. *J. Mater. Chem. A* **2016,** *4*, 17686.

32. Viter, R.; Iatsunskyi, I.; Fedorenko, V.; Tumenas, S.; Balevicius, Z.; Ramanavicius, A.; Balme, S.; Kempiński, M.; Nowaczyk, G.; Jurga, S.; Bechelany, M. Enhancement of Electronic and Optical Properties of Zno/Al2o3nanolaminate Coated Electrospun Nanofibers. *The Journal of Physical Chemistry C* **2016,** *120*, 5124-5132.

33. Shirley, D. A. High-Resolution X-Ray Photoemission Spectrum of the Valence Bands of Gold. *Phys. Rev. B* **1972,** *5*, 4709.

34. Scofield, J. H. Hartree-Slater Subshell Photoionization Cross-Sections at 1254 and 1487 Ev. *Journal of Electron Spectroscopy and Related Phenomena* **1976,** *8*, 129-137.

35. Jung, K. W.; Park, D. S.; Hwang, M. J.; Ahn, K. H. Decolorization of Acid Orange 7 by an Electric Field-Assisted Modified Orifice Plate Hydrodynamic Cavitation System: Optimization of Operational Parameters. *Ultrason Sonochem* **2015,** *26*, 22-9.

36. Ruiz, E. J.; Hernández-Ramírez, A.; Peralta-Hernández, J. M.; Arias, C.; Brillas, E. Application of Solar Photoelectro-Fenton Technology to Azo Dyes Mineralization: Effect of

Current Density, Fe2+ and Dye Concentrations. *Chemical Engineering Journal* **2011,** *171*, 385-392.

37.   Drobek, M.; Bechelany, M.; Vallicari, C.; Abou Chaaya, A.; Charmette, C.; Salvador-Levehang, C.; Miele, P.; Julbe, A. An Innovative Approach for the Preparation of Confined Zif-8 Membranes by Conversion of Zno Ald Layers. *Journal of Membrane Science* **2015,** *475*, 39-46.

38.   Bechelany, M.; Drobek, M.; Vallicari, C.; Abou Chaaya, A.; Julbe, A.; Miele, P. Highly Crystalline Mof-Based Materials Grown on Electrospun Nanofibers. *Nanoscale* **2015,** *7*, 5794-802.

39.   Alexeyeva, N.; Shulga, E.; Kisand, V.; Kink, I.; Tammeveski, K. Electroreduction of Oxygen on Nitrogen-Doped Carbon Nanotube Modified Glassy Carbon Electrodes in Acid and Alkaline Solutions. *Journal of Electroanalytical Chemistry* **2010,** *648*, 169-175.

40.   Yu-Xiao Zhou; Yu-Zhen Chen; Lina Cao; Junling Lu; Jiang, H.-L. Conversion of a Metal–Organic Framework to N-Doped Porous Carbon Incorporing Co and Coo Nanoparticles. Direct Oxidation of Alcohols to Esters. *Chem. Commun* **2015,** *51*, 8292.

41.   Tang, J.; Salunkhe, R. R.; Liu, J.; Torad, N. L.; Imura, M.; Furukawa, S.; Yamauchi, Y. Thermal Conversion of Core-Shell Metal-Organic Frameworks: A New Method for Selectively Functionalized Nanoporous Hybrid Carbon. *J Am Chem Soc* **2015,** *137*, 1572-80.

42.   Chao, S.; Zou, F.; Wan, F.; Dong, X.; Wang, Y.; Guan, Q.; Wang, G.; Li, W. Nitrogen-Doped Carbon Derived from Zif-8 as a High-Performance Metal-Free Catalyst for Acetylene Hydrochlorination. *Sci Rep* **2017,** *7*, 39789.

43.   Eren, Z.; Acar, F. N. Adsorption of Reactive Black 5 from an Aqueous Solution: Equilibrium and Kinetic Studies. *Desalination* **2006,** *194*, 1-10.

44.   Nagarethinam Kannan; Sundaram, M. M. Kinetics and Mechanism of Removal of Methylene Blue by Adsorption on Various Carbons—a Comparative Study. *Dyes and Pigments* **2001,** *51*, 25-40.

45.   Lim, C. K.; Bay, H. H.; Neoh, C. H.; Aris, A.; Abdul Majid, Z.; Ibrahim, Z. Application of Zeolite-Activated Carbon Macrocomposite for the Adsorption of Acid Orange 7: Isotherm, Kinetic and Thermodynamic Studies. *Environ Sci Pollut Res Int* **2013,** *20*, 7243-55.

46.   Moussavi, G.; Mahmoudi, M. Removal of Azo and Anthraquinone Reactive Dyes from Industrial Wastewaters Using Mgo Nanoparticles. *J Hazard Mater* **2009,** *168*, 806-12.

47.   Lin, J.; Zhan, Y. Adsorption of Humic Acid from Aqueous Solution onto Unmodified and Surfactant-Modified Chitosan/Zeolite Composites. *Chemical Engineering Journal* **2012,** *200-202*, 202-213.

48.   Sathishkumar, P.; Arulkumar, M.; Palvannan, T. Utilization of Agro-Industrial Waste Jatropha Curcas Pods as an Activated Carbon for the Adsorption of Reactive Dye Remazol Brilliant Blue R (Rbbr). *Journal of Cleaner Production* **2012,** *22*, 67-75.

49.   Hammami, S.; Bellakhal, N.; Oturan, N.; Oturan, M. A.; Dachraoui, M. Degradation of Acid Orange 7 by Electrochemically Generated (*)Oh Radicals in Acidic Aqueous Medium Using a Boron-Doped Diamond or Platinum Anode: A Mechanistic Study. *Chemosphere* **2008,** *73*, 678-84.

50.   Pajootan, E.; Arami, M.; Rahimdokht, M. Discoloration of Wastewater in a Continuous Electro-Fenton Process Using Modified Graphite Electrode with Multi-Walled Carbon Nanotubes/Surfactant. *Separation and Purification Technology* **2014,** *130*, 34-44.

51.   Z.H. Sheng; L. Shao; J.J. Chen; W.J. Bao; F.B. Wang; X.H. Xia Synthesis of Nitrogen-Doped Graphene Via Thermal Treatment of Graphene Oxide within Methylimidazole and Its Capacitance Performance as Electric Double Layer Capacitor. *ACS Nano* **2011,** *5*, 4350.

52.   Mousset, E.; Ko, Z. T.; Syafiq, M.; Wang, Z.; Lefebvre, O. Electrocatalytic Activity Enhancement of a Graphene Ink-Coated Carbon Cloth Cathode for Oxidative Treatment. *Electrochimica Acta* **2016,** *222*, 1628-1641.

TOC Graphic